

Self-powered pulsed direct current stimulation system for enhancing osteogenesis in MC3T3-E1

Yingzi Zhang^{a,1}, Lingling Xu^{b,d,1}, Zhuo Liu^{b,c,1}, Xi Cui^{b,d}, Zhuo Xiang^{b,f}, Jinyu Bai^a, Dongjie Jiang^{b,d}, Jiangtao Xue^{b,h}, Chan Wang^{b,d}, Youxi Lin^g, Zhe Li^{b,h}, Yizhu Shan^{b,d}, Yuan Yang^{b,d}, Lin Bo^{e,*}, Zhou Li^{b,d,f,*}, Xiaozhong Zhou^{a,**}

^a Department of Orthopaedics, the Second Affiliated Hospital of Soochow University, Jiangsu 215004, China

^b CAS Center for Excellence in Nanoscience Beijing Key Laboratory of Micro-nano Energy and Sensor, Beijing Institute of Nanoenergy and Nanosystems, Chinese Academy of Sciences, Beijing 101400, China

^c Beijing Advanced Innovation Centre for Biomedical Engineering Key Laboratory for Biomechanics and Mechanobiology of Ministry of Education School of Biological Science and Medical Engineering Beihang University, Beijing 100191, China

^d School of Nanoscience and Technology, University of Chinese Academy of Sciences, Beijing 100049, China

^e Department of Rheumatology, the Second Affiliated Hospital of Soochow University, Jiangsu 215004, China

^f Center of Nanoenergy Research School of Physical Science and Technology Guangxi University, Nanning 530004, China

^g Department of Orthopedic Surgery, Beijing Tiantan Hospital, Capital Medical University, Beijing 100050, China

^h Institute of Engineering Medicine, Beijing Institute of Technology, Beijing 100081, China

ARTICLE INFO

Keywords:

Electrical stimulation
Pulsed direct current
Self-powered
Nanogenerator
Osteoblast

ABSTRACT

Promoting the differentiation of osteoblasts is critical to maintain bone homeostasis for treatment osteoporosis and fracture healing. For these orthopedic diseases, a portable, highly patient compliance therapy device remains a great challenge. Here, we proposed a biomechanical-energy-driven shape memory piezoelectric nanogenerator (sm-PENG) that integrated with fixation splint to promote osteogenic differentiation. The pulsed direct current (DC) generated from the sm-PENG effectively promote MC3T3-E1 preosteoblast cell proliferation, orientation and increase intracellular calcium ion. At the same time, the ALP activity of cells is also improved by pulsed-DC under long-term culture conditions. Ultimately, increasing calcium deposition, extracellular matrix mineralization and osteogenesis. Our work demonstrates the potential of sm-PENG as a power source for pulsed-DC stimulation of bone repair, and shows great prospect self-powered and portable electronic medical device.

1. Introduction

Bone has the function of sports, support, and protection of the body, which is of great significance to maintain the normal activities of the human. Bone fracture is a common clinical disease that causes the continuity of bone structure to be completely or partially broken [1]. It mostly occurs in children and the elderly [2]. The healing process of fracture will continue for a long time, and susceptible to the interference of many factors leading to delayed or even non-healing, which seriously affects the quality of life of patients. Therefore, how to promote fracture repair and shorten the healing time is the frontier and difficult point of orthopedics research.

With in-depth study on the mechanism of fracture healing, A variety of adjuvant treatments have been widely used clinically. For example, bone tissue engineering (BTE) simulates bone autograft in many aspects, uses scaffolds, bone-forming cells to fill the defect bone, and regulation of cell-cell and cell-scaffold interaction by adding growth factors or electrical stimulation [3,4]. Especially the physical therapy of electrical stimulation, its effect of promoting fracture healing has been fully confirmed. Electrical stimulation can not only promote the healing of fresh fractures, but also has a good effect on delayed healing of fractures, nonunion, osteotomy and false joint formation [5,6].

Electrical stimulation for enhance osteogenesis that is a critical factor in the process of bone remodeling repair process. It can be divided into

* Corresponding authors.

** Corresponding author at: Department of Orthopaedics, the Second Affiliated Hospital of Soochow University, Jiangsu 215004, China.

E-mail addresses: bolin@suda.edu.cn (L. Bo), zli@binn.cas.cn (Z. Li), zhouxz@suda.edu.cn (X. Zhou).

¹ These authors contributed equally to this work.

current stimulation [7–9], electric and electromagnetic field stimulation [10–12]. However, during clinical treatment, the electrical stimulation device is too bulky. A portable, highly patient compliance electrical stimulation therapy device for bone repair remains a great challenge. Portable and new self-powered electrical stimulation devices based on nanogenerator that are constantly being proposed [13,14]. The nanogenerator technology including triboelectric nanogenerator [15,16] and piezoelectric nanogenerator [17,18], which can convert the biomechanical energy to electricity. With the continuous improvement of output performance of nanogenerator [19], high-stability, low-cost, light-weight and easy fabricated nanogenerators have shown great potential in biomedical engineering filed for electrical stimulation [20] and biosensor [21], including drug delivery, cancer treatment [22,23], wound healing [24], nerve stimulation [25,26], muscle stimulation [27] and health monitoring, etc [28–31]. It has also received a lot of attention in the field of bone healing [32,33]. But at present, only the results of electric field stimulation have been reported. As a common clinical method, the effect of current stimulation based on nanogenerator has not been reported. The specific mechanism of current stimulation promoting bone healing has not been clarified. Compared with the electric field, it only needs a small current to directly effect on the deep bone tissue, and the device is more portable, which has a good clinical application prospect.

Here, we construct an integrated self-powered pulsed-DC stimulation device based on shape memory piezoelectric nanogenerator and fracture fixation splint used for bone repair. A shape-memory piezoelectric nanogenerator (sm-PENG) is demonstrated. The short-circuit current can reach 20 μA by tapping, which is more than twice that of the flat structure. In addition, the sm-PENG can integrate with fixation splint to form an electrical stimulation therapy system for osteoblast differentiation, which has good flexibility and portability. The pulse-DC generated by the sm-PENG through the rectifier bridge can effectively promote cell proliferation, intracellular calcium ion, which has a certain cell orientation effect. At the same time, it can promote the ALP activity of cells under long-term culture conditions, ultimately promote calcium deposition, extracellular matrix mineralization and osteogenic differentiation. The biological effect of pulsed-DC stimulation from the sm-PENG is basically consistent with that of the commercial signal generator. This work provides a new idea for fracture healing and promote the progress of nanogenerator's application in wearable electric medical devices.

2. Material and methods

2.1. The fabrication of sm-PENG

First, the Kapton film with the size of $55 \times 25 \times 0.1 \text{ mm}^3$ was thermo forming around $200 \text{ }^\circ\text{C}$ by the heating rod. After forming, the PVDF film coated with the Ag electrodes ($50 \times 20 \times 0.11 \text{ mm}^3$) was attached to the arched Kapton film. Then, the PET film was employed as a packaged layer to encapsulate the device. Finally, all parts were glued together via silicone polymers one by one for fabricating the sm-PENG.

2.2. The output characterization of sm-PENG

A linear motor (LinMot, E100) with periodical mechanical triggering was employed to drive the sm-PENG. The output performance of the sm-PENG was characterized by a Keithley 6517 electrometer and an oscilloscope (LeCoy, HDO6104). An ESM301/Mark-10 system was used for applying and detecting the force.

2.3. Preparation of electrical stimulation device

Indium tin oxide (ITO) deposited on the glass ($1.5 \times 3 \text{ cm}^2$) was used as the conductive substrate. The cylinder with an internal diameter of 6 mm was printed with thermoplastic PLA material by the 3D printer and

six cylinders were fixed on a conductive substrate by PDMS. The copper tape was used to fix copper wires on both sides of the substrate. The glass device with cylinder and wire was put into a six-well plate, the photo of the device was shown in Fig. S1. The plates were soaked in 75% ethanol for 3 h, cleaned with sterile water and irradiated with ultraviolet light in laminar chamber for 1 h. Then the cylinder was soaked in L-polylysine solution for 1 h, and dry overnight for cell culture.

2.4. Cell culture and differentiation

Murine calvarial preosteoblasts (MC3T3-E1, ATCC CRL-2594) were seeded in the cylinder with 8000 cells/ cm^2 and cultured in complete α -MEM (Minimum Eagle's Medium) containing 10% fetal bovine serum and 1% penicillin-streptomycin with 5% CO_2 at $37 \text{ }^\circ\text{C}$. After 12 h of culture, cells were cultured with the induced culture medium adding 0.01 mmol/L dexamethasone (Dex), 10 mmol/L β -sodium glycerophosphate, and 0.5 mmol/L ascorbic acid to induce cell differentiation.

2.5. Electrical stimulation of MC3T3-E1

There are two kinds of electrical stimulation systems including signal generator electrical stimulation and sm-PENG electrical stimulation system. The whole electrical stimulation system consists of three parts: stimulation power supply, rectifier bridge and cell culture device. Signal generator and Linear motor driven PENG were used as the power supply. The electrical stimulation parameters of the signal generator were 20 μA sine wave, and those of PENG were 20 μA pulse wave, with the frequency of 3 Hz. The cells were exposed to current stimulation for 2 h per day.

2.6. Evaluation of cell morphology, alignment, proliferation, and migration

The cells were cultured and stimulated for 1, 2 and 3 days and the cell proliferation level were evaluated by Cell Count Kit-8 (CCK-8, Dojindo Molecular Technologies, Inc. Japan). After removing the culture medium and wash it with phosphate-buffered saline solution (PBS), add 110 μL complete medium including 10 μL CCK-8 reagent. After incubation for 2 h, transfer 150 μL culture supernatant into 96 well plate and measure the absorbance at 450 nm. To visualize the cytoskeleton and nucleus, F-actin (green) and nucleus acids (blue) were stained with phalloidin and Hoechst. Before staining, the cells were washed with PBS three times. Then cells were fixed with fixative for 10 mins and stained with phalloidin for 40 mins at room temperature. Finally, Hoechst was added and incubated for 10 mins, each of the described steps was followed by PBS washing three times. The stained cells were visualized by laser scanning confocal microscope (Leica SP8). To statistic the directionality of cell arrangement, we randomly selected 10 photographs per group and measuring the angle of 10 cells per group. The sharp angle between actin direction and horizontal direction was recorded as β by ImageJ. Every tenth degree was the interval for statistical analysis. Cell migration was characterized by wound healing assays, cells were seeded into ITO substrate and allowed to grow to 90% confluency. Scratches were generated with a 200 μL pipette tip and washed with PBS to form cell-free wounds. Then the cells were incubated with an induced medium with stimulated for 24 h continuously. No electrical stimulation group was used as the control group. The cells at the same position were photographed and recorded every 6 h, and then the cell migration rate was calculated by ImageJ.

2.7. Measurement of intracellular calcium levels

Intracellular calcium levels in cells were measured with Fluo-4 direct calcium assay kits (Molecular Probes™, Thermo Fisher Scientific) after one day and three days of electrical stimulation. After removing the culture medium from the wells, adding 100 μL of the $1 \times$ Fluo-4 Direct

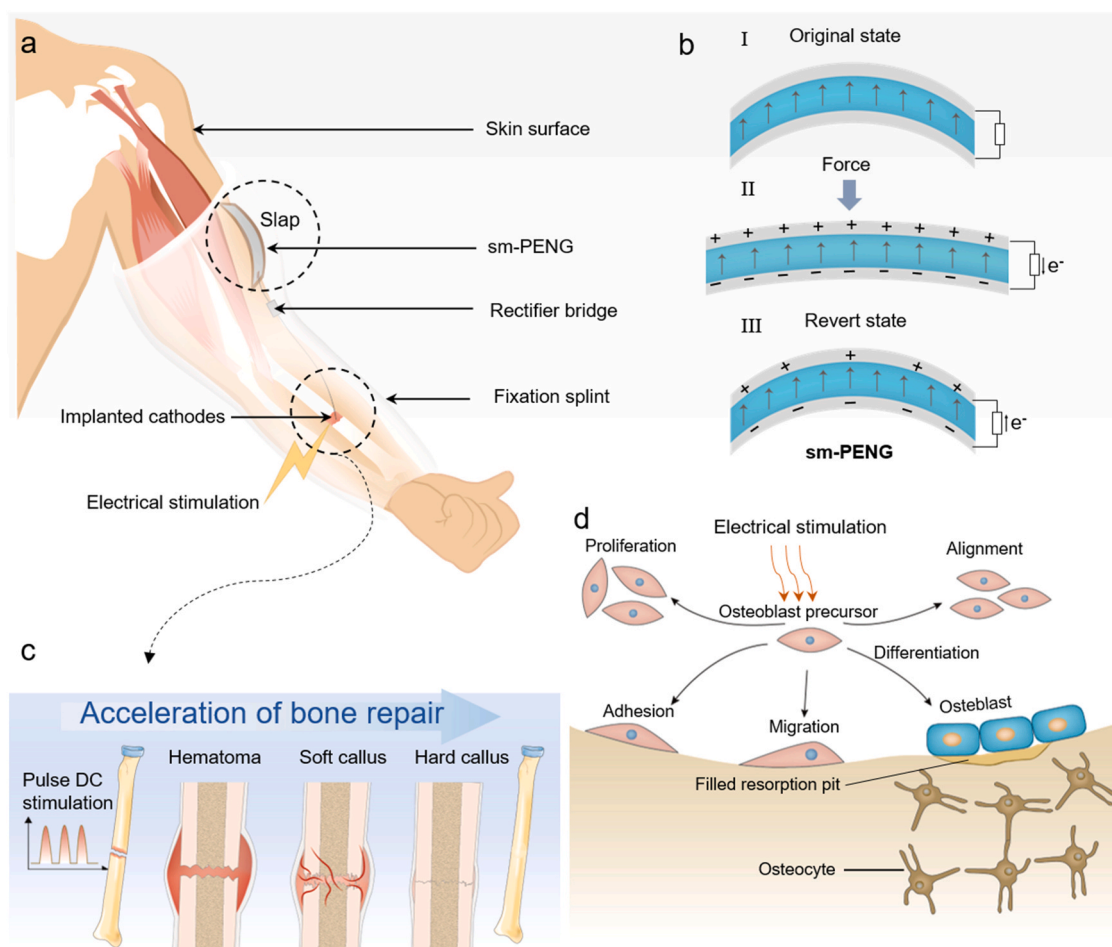


Fig. 1. The Schematic diagram of self-powered electrical stimulation for bone repair. a) Schematic of the integrated self-powered pulsed-DC device based on sm-PENG and fracture fixation splint for bone repair in vivo. b) Working principle of the PVDF piezoelectric layer. c) Electrical stimulation accelerates bone repair. d) Effect of electrical stimulation on osteoblast precursor behavior.

calcium reagent loading solution per well and incubate plates at 37 °C for 60 mins. The stained cells were viewed by laser scanning confocal microscope (Leica SP8). Similarly, stained cells were washed with PBS, digested with trypsin, centrifuged, and collected. Each well was resuspended with 100 PBS, and measured by flow cytometry at 488 nm.

2.8. Alkaline phosphatase staining and activity measurement

Seven days after electrical stimulation, an alkaline phosphatase staining kit (Solarbio Science & Technology Co., Ltd. Beijing, China) was used for staining. The cultured cells were washed with PBS and fixed with ALP fixative for 3 mins. After a wash with PBS three times, 100 μ L ALP incubation solution was added and incubate in dark for 20 mins and stained for 3 mins with nuclear solid red staining solution. Alkaline phosphatase (AKP/ALP) activity assay kit (Solarbio Science & Technology Co., Ltd. Beijing, China) was used to detect the alkaline phosphatase activity of the cells after 7 and 14 days of electrical stimulation. After digestion, the cells were centrifuged and each well was resuspended with 100 μ L sterile deionized water. The cells were repeatedly frozen and thawed at - 80 °C for 3 times with an interval of 30 mins. After centrifugation, ALP activity in the supernatant was determined. The total protein concentration of cells was calculated from standard curves of BSA by Bradford method. Fig. S6 presented the standard curve of the protein quantitative test. The ALP activity was normalized to the protein concentration.

2.9. Alizarin red staining

Alizarin red staining was performed after 18 days of electrical stimulation to determine the presence of extracellular matrix mineralization. Cells were washed three times with PBS and were fixed for 15 mins and washed with deionized water for three times. After that, the cells were attained with alizarin red staining solution at room temperature for 30 mins and take pictures under the microscope. The average integrated optical density (IOD) was analyzed by Image-Pro Plus.

2.10. Statistical analysis

All data were present as mean \pm standard deviations of are presentative of at least three parallel samples. One-way and two-way ANOVA were used to determine the significant differences among the groups and a statistical significance was assigned as * $P < 0.05$, ** $P < 0.01$, *** $P < 0.001$.

3. Results and discussion

3.1. Overview of the self-powered pulsed-DC stimulation system

We construct an integrated self-powered pulsed-DC stimulation device based on shape memory piezoelectric nanogenerator with arch structure and fracture fixation splint used for bone repair (Fig. 1a). The sm-PENG exhibiting flexibility and portability can be well integrated with the fixation splint, simply fixed both ends of the sm-PENG on the

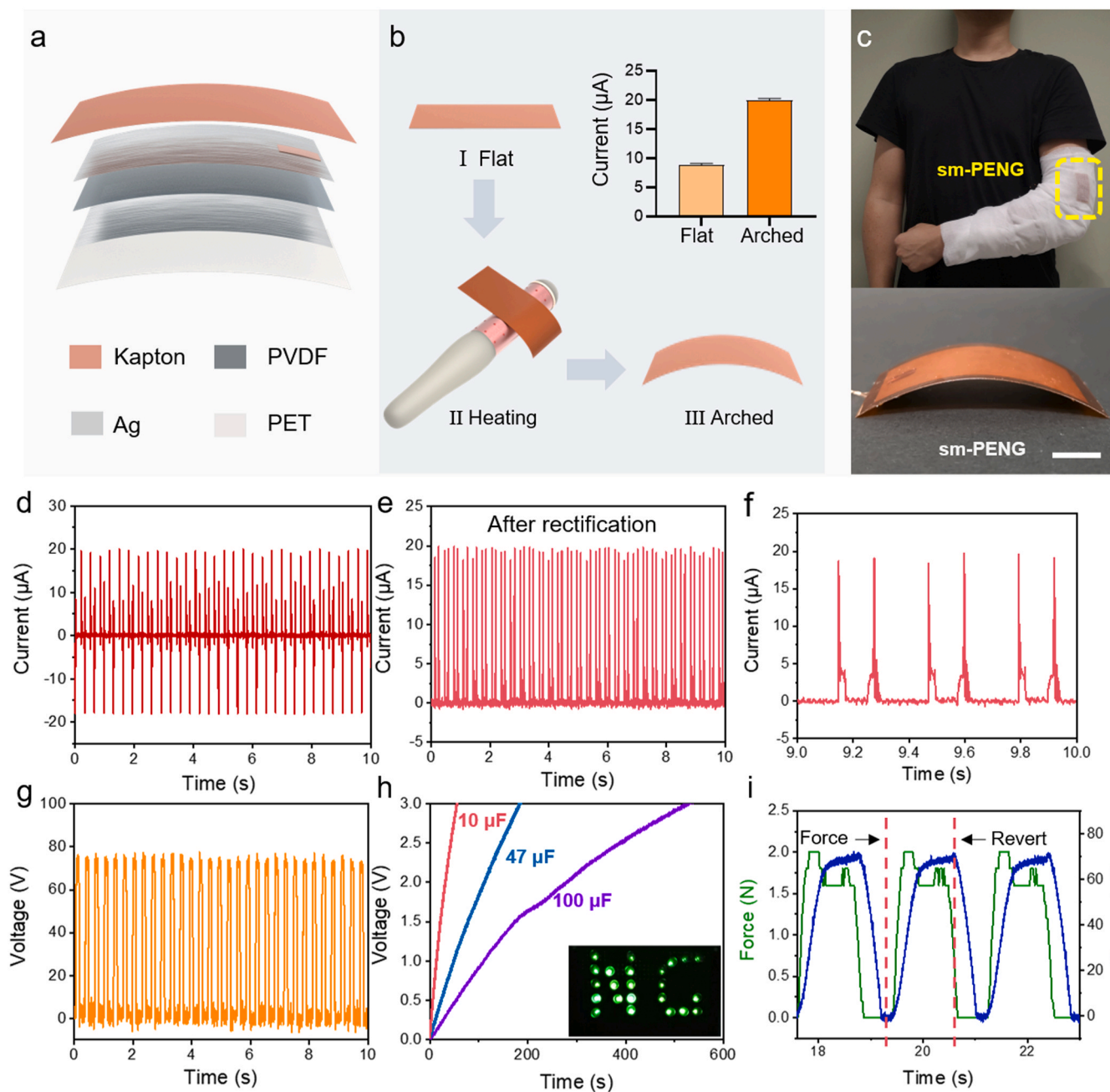


Fig. 2. Preparation and characterization of sm-PENG. a) The schematic structure of the sm-PENG. b) Kapton film was processed by thermo forming technology to realize arch structure and the short-circuit current of the device before and after thermo forming. c) The photograph of sm-PENG and integrated with a fixation splint. Scale bar: 1 cm. d) Short-circuit current of the sm-PENG. e) The short-circuit current after rectification. f) Local amplification of short circuit current. g) The open-circuit voltage of the sm-PENG. h) The charging profile of three different specifications of and the sm-PENG could directly power 23 LEDs. i) The profile of force-electricity coupling test.

gauze with adhesive tape. Fig. 1b shows the working principle of the sm-PENG. In the original arched state, the electric dipoles in PVDF were arranged in the electrode direction. When the device is flattened down by a force, the polarization charge density increases to generate an electric field and electrons flow through the external load. When the force was eliminated, the electrons would flow in the opposite direction. The pulsed alternating current generated by gently tapping sm-PENG that is converted into pulsed-DC through the rectifier bridge, and the electrode is implanted in the fracture site for electrical stimulation of bone repair. The healing process is physiologically complex and can be divided into hematoma, soft callus and hard callus (Fig. 1c). Osteogenesis is involved in bone remodeling in the repair process, there are a

large number of studies have shown that electrical stimulation could enhance osteogenesis and bone repair. but the specific mechanism of current stimulation promoting bone healing has not been clarified. but many previous works have found that it has significant effects on the proliferation, adhesion, migration, directional arrangement, differentiation, and other aspects of osteoblast precursor cells (Fig. 1d) [29]. Importantly, all of these behaviors have a potential role in promoting bone repair by electrical stimulation.

3.2. Characterization of sm-PENG

The as-fabricate sm-PENG was composed of piezoelectric layer,

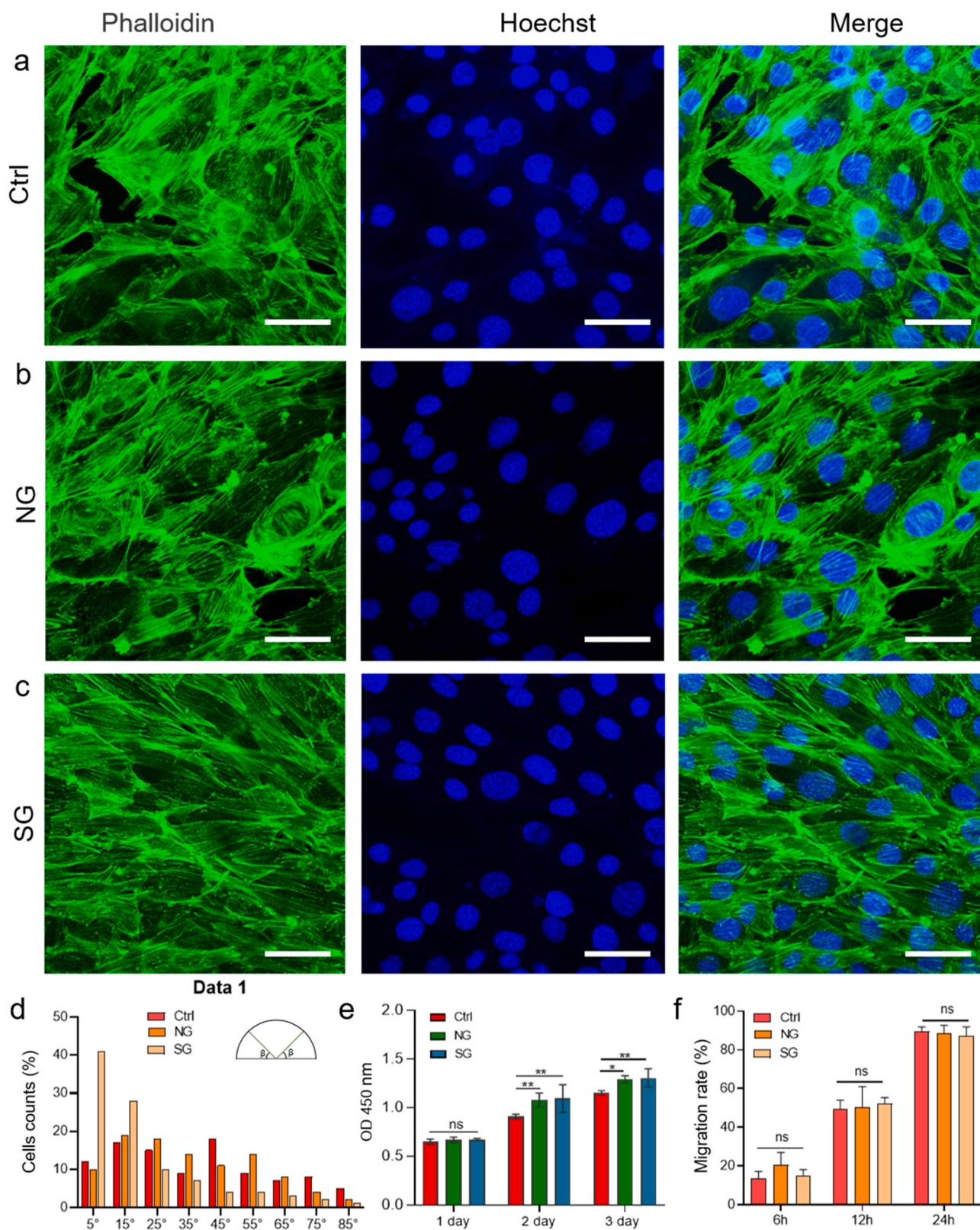


Fig. 3. Morphology, proliferation and migration of MC3T3-E1 cell under the pulsed-DC stimulation. (a–c) Fluorescence image of cellular filamentous actin (phalloidin, green) and nucleus (Hoechst, blue) three days after electrical stimulation. d) Cell alignment analysis after electrical stimulation for three days. e) MC3T3-E1 cell viability determined by the CCK-8 assay. Compared with the ctrl group. f) Migration rate of MC3T3-E1 after 24 h electrical stimulation. The scale bar is 50 μ m.

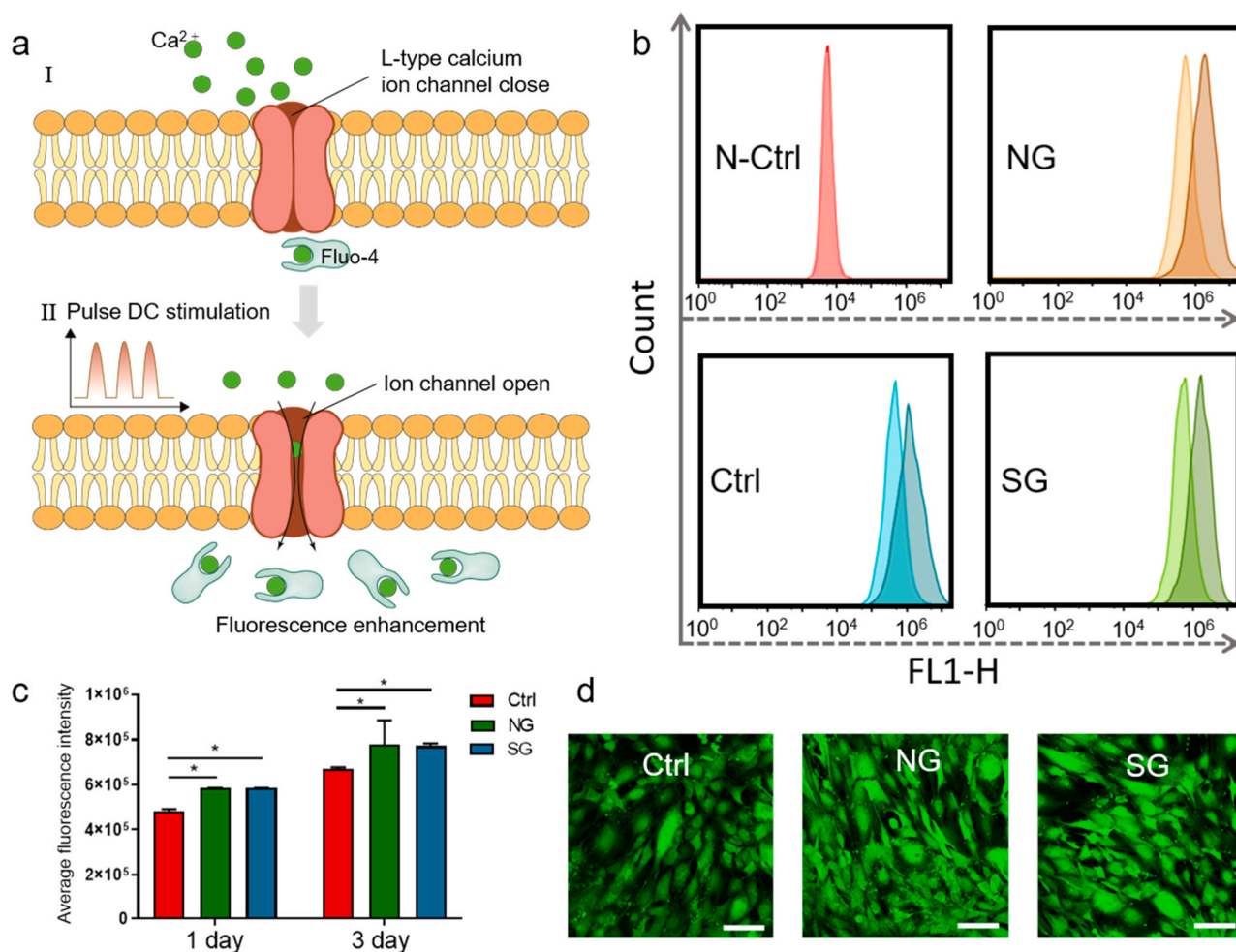


Fig. 4. The intracellular calcium ion level after different electrical stimulation times. a) Schematic of intracellular calcium concentration promoted by electrical stimulation, calcium ion concentration was characterized by fluorescence staining. b) Compare the intracellular Ca^{2+} was measured by flow cytometer in the same group after EF stimulated in 1 day and 3 days. Unstained cells were used as N-Ctrl. c) The average fluorescence intensity was recorded from average FL1-H. d) The optical fluorescence diagrams of MC3T3-E1 cells staining by Fluo-4 after current stimulated for 2 h. Scale bar: 100 μ m.

substrate, and electrodes, which were packaged by PET film. Fig. 2a displays the schematic structure of the sm-PENG. The PVDF film as piezoelectric layer coated with Ag that was attached on the Kapton film, which serves as a substrate. Besides, it is worth noting that the Kapton film was processed by thermo forming technology to realize arch structure for its excellent elasticity and strength (Fig. 2b). This process guarantees the deformation of PVDF film more effective for enhancing the stress and strain of the device in operation, which will ultimately increase the output performance of the device. As result, the short-circuit current of the device increased from 8.2 μ A to 20 μ A after thermo forming. This thin-film device with a total dimension of $55 \times 25 \times 0.3$ mm³ can be integrated with a fixation splint to achieve portable treatment for clinical use (Fig. 2c). The output performance was characterized by laboratory conditions. Fig. 2d exhibits the short-circuit current of the sm-PENG, the short-circuit current value has no decay with about 20 μ A after rectification (Fig. 2e and 2f). The open-circuit voltage of the sm-PENG was also examined, with about 78 V (Fig. 2g). Compared with the initial state after 10,000 working cycles, the I_{sc} of sm-PENG remained stable (Fig. S2, Supporting Information), showing good durability. To prove the ability of the sm-PENG as a power source, we further evaluated the charging ability of the device. Three different specifications of capacitors can be well charged from 0 V to 3 V within 600 s, and the sm-PENG could directly power 23 LEDs (Fig. 2h). Video S1 visually represented the current generated from sm-PENG with a slight tap. Through the force-electricity coupling test system, the

relationship between the force application process and the electrical output signal of the sm-PENG is shown in Fig. 2i. The output of the sm-PENG continues to increase with force loading. When the force loading drops to zero, the output of the sm-PENG begins to fall back due to its own resilience. The force to flatten the sm-PENG is about 2N. At this time, the device can achieve the optimal output performance. As a wearable device, the sm-PENG will achieve considerable mechanical energy-to-electricity conversion efficiency by tapping lightly.

Supplementary material related to this article can be found online at [doi:10.1016/j.nanoen.2021.106009](https://doi.org/10.1016/j.nanoen.2021.106009).

3.3. The effect of electrical stimulation on cell morphology, alignment, proliferation, and migration

Cell electrical stimulation system mainly includes power supply system, rectifier bridge and cell culture device. When electrical stimulation was applied, the current density on ITO surface and in the culture medium was simulated by finite element analysis. The instantaneous current density on ITO surface can reach 350 μ A/cm² (Fig. S3). As shown in Fig. 3a, after three days of stimulation, the cells fully extend along the main axis on the basement after adherent, the cells in the nuclear area were wider and narrower at both ends, and form multiple foot like bifurcations, which may be related to cell exclusion and communication. With the increase of culture time, the number of osteoblasts increased and multi-layer cells were formed. (Fig. S4) Cell

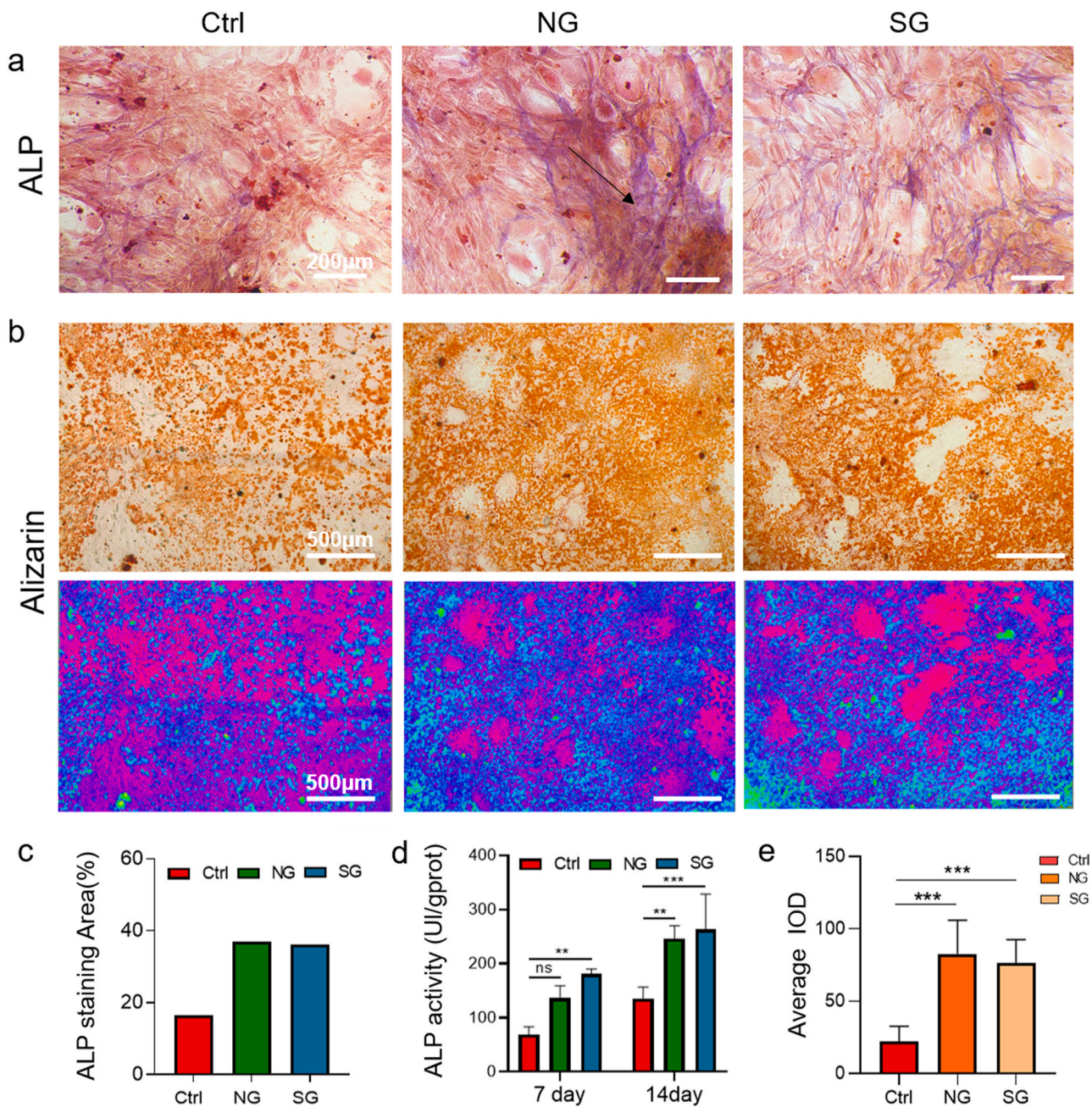


Fig. 5. Evaluation of osteogenic differentiation after electrical stimulation. Untreated MC3T3-E1 cells were used as control. a) ALP staining was performed 14 days after electrical stimulation activity. b) Alizarin red S staining was used to visualize the level of mineralization 18 days after electrical stimulation. c) The percentage of ALP staining area was recorded from image a. d) ALP activities were measured on day 7 and day 14 after electrical stimulation. e) The average integral optical density (IOD) of the cell was quantified using Image-Pro Plus. ($n = 6$).

alignment relative to the current was analyzed using ImageJ. The acute angle between the long axis of the cell and the horizontal line was recorded as β , 86% of the cells in the SG group had a β value less than 40° , which was 53% in the control group and 61% in the NG group. These results indicate that current stimulation can promote the directional arrangement of cells. Osteoblast cell proliferation and migration are directly associated with bone repair. On the first day of stimulation, there was no significant difference in cell proliferation among different groups, but on the second and third days, the proliferation rate of the NG and SG group was significantly higher than the control group, there was no significant difference between the SG and NG group (Fig. 3e). As shown in Figs. 3f and S5, compared with the control group, the cell migration rate of the experimental group had no significant difference,

indicating that short-term continuous pulsed-DC stimulation does not increase cell migration rate.

3.4. Intracellular calcium ion level

Many studies have found that calcium plays an important role in the response of bone cells to electric stimulation. ES can increase the concentration of intracellular calcium ion in two ways, the first is the release of calcium from the intracellular calcium pool, and the second is to open the L-type calcium ion channel through transmembrane potential depolarization to make extracellular calcium influx into cells (Fig. 4a) [34]. Cytoplasmic calcium can directly activate protein kinase or indirectly activate protein kinase-related pathway by activating calmodulin,

which converts the electric signal into biological signal and transmits it to cells, causing gene expression and protein synthesis and promoting cell proliferation and differentiation. The intracellular calcium flow was analyzed by flow cytometry after one and three days of stimulation. The results showed that the intracellular calcium level was increased with the increase of stimulation time under the same experimental conditions (Fig. 4b). At the same time, the intracellular calcium content in the electrical stimulation group was significantly higher than that in the control group (Fig. 4c). Fig. 4d shows the calcium fluorescence image of MC3T3-E1. Due to the effect of the fluorescent probe, the cell adhesion is reduced, and the cell tends to be round with the edge smooth, but the intercellular connection is still clear. Compared with the control group, the fluorescence intensity of the electrical stimulation groups were also significantly enhanced.

3.5. ALP activity and extracellular matrix mineralization

The expression of alkaline phosphatase is an important marker of osteoblast differentiation in the early stage. The highest activity was found in the late proliferation stage, which provided favorable conditions for phosphate enrichment in the mineralization stage [35]. The degree of osteoblast differentiation can be characterized by ALP activity. ALP staining was applied by the azo coupling method on the 14th day of electrical stimulation. The results are shown in Fig. 5a. The purple part (black arrow) is cells that had ALP activity, indicating that they have differentiated into osteoblasts. We used ImageJ to calculate the area of the purple part, the results are shown in Fig. 5c. The area of ALP staining in the experimental group is more than twice that in the control group. The staining of the NG group was much deeper than that of the SG group, but there was no significant difference in the staining area. We also used a quantitative method to detect ALP activity on 7 and 14 days. With the extension of culture time, ALP activity increased more significantly than that of the control group. ALP activity increased more significantly than that of the control group. On the seventh day, the ALP activity of the SG group was significantly higher than that of the control group, and that of the NG group was also higher than the control group, but the difference was not significant. On the 14th day of ES, there were significant differences between the two experimental groups and the control group, indicating that pulsed-DC electrical stimulation could enhance ALP activity (Fig. 5d).

Extracellular matrix mineralization is the most direct manifestation of osteogenesis [36]. After 18 days of electrical stimulation, the level of mineralization was analyzed using alizarin red S staining. The orange-red particles in the first line of Fig. 5b are calcium phosphate crystals deposited after staining, to distinguish the coloring situation more intuitively, three groups of images were processed by Image J software (second line). It is shown that the coloring area (blue) of the experimental group was significantly larger than that of the control group. Further analysis of the average optical density also showed that the extracellular matrix mineralization was more obvious in the electrical stimulation group. The pulse electricity generated from sm-PENG and signal generator can obviously promote osteogenic differentiation.

4. Conclusions

In summary, we developed a sm-PENG processed by thermo forming technology to realize arch structure with the short-circuit current of 20 μ A, which is more than twice that of the flat structure. It can be integrated with fixation splint to form an electrical stimulation therapy system for promoting osteoblast differentiation with good flexibility and portability. The sm-PENG and commercial signal generator were used for osteogenic differentiation in vitro. The biological effect of sm-PENG pulsed-DC stimulation from the sm-PENG is basically consistent with that of the commercial signal generator. Under the stimulation of 3 Hz, 20 μ A, two hours per day, the results showed that at the early stage of differentiation, pulsed-DC stimulation could promote the proliferation

of MC3T3-E1 cells, enhance the intracellular calcium concentration, and had no obvious effect on cell migration. In the middle and late stages of differentiation, the electrical stimulation can enhance ALP activity, promote extracellular matrix mineralization and accelerated osteogenic. It demonstrated that self-powered pulsed-DC stimulation is promising for bone repair, and shows great prospect self-powered and portable electronic medical device.

CRedit authorship contribution statement

Y.Z.Z., L.L.X. and Zhuo. L performed experimental measurements, data curation and wrote the manuscript. X.C., Z.X., J.Y.B., Zhe L., Y.Z.S. and Y.Y. accomplished the material characterization and directed the preparation of device. J.T.X. complete COMSOL simulation. C.W., D.J.J. and Y.X.L. draw graphics, L.B., Zhou L. and X.X.Z. put forward the plan, provide experimental conditions, revise the article, and guided the work.

Declaration of Competing Interest

The authors declare that they have no known competing financial interests or personal relationships that could have appeared to influence the work reported in this paper.

Acknowledgments

This study was financially supported by the National Key R&D project from Minister of Science and Technology, China (2016YFA0202703), National Natural Science Foundation of China (61875015, 81873995, 81902207, 81171712), Beijing Natural Science Foundation (JQ20038), Science and Technology Planning Project of Guangdong Province (2018B030331001), China Postdoctoral Science Foundation (2020M680302), Key laboratory of spinal cord injury repair of Suzhou (SZS201807), the Suzhou Young Science and Technology Project (KJXW2018012), the Fundamental Research Funds for the Central Universities.

Appendix A. Supporting information

Supplementary data associated with this article can be found in the online version at doi:10.1016/j.nanoen.2021.106009.

References

- [1] T.A. Einhorn, L.C. Gerstenfeld, Fracture healing: mechanisms and interventions, *Nat. Rev. Rheumatol.* 11 (2015) 45–54.
- [2] J.E. Compston, M.R. McClung, W.D. Leslie, Osteoporosis, *Lancet* 393 (2019) 364–376.
- [3] R. Dimitriou, E. Jones, D. McGonagle, P.V. Giannoudis, Bone regeneration: current concepts and future directions, *BMC Med.* 9 (2011) 66.
- [4] H.Y. Lin, K.H. Lu, Repairing large bone fractures with low frequency electromagnetic fields, *J. Orthop. Res.* 28 (2010) 265–270.
- [5] T. Yoshida, W.C. Kim, T. Kubo, Bone fracture and the healing mechanisms. Fracture treatment using electrical stimulation, *Clin. Calcium* 19 (2009) 709–717.
- [6] B.W. Kooistra, A. Jain, B.P. Hanson, Electrical stimulation: nonunions, *Indian J. Orthop.* 43 (2009) 149–155.
- [7] J. Zhang, K.G. Neoh, X. Hu, E.-T. Kang, W. Wang, Combined effects of direct current stimulation and immobilized BMP-2 for enhancement of osteogenesis, *Biotechnol. Bioeng.* 110 (2013) 1466–1475.
- [8] S. Bodhak, S. Bose, W.C. Kinsel, A. Bandyopadhyay, Investigation of in vitro bone cell adhesion and proliferation on Ti using direct current stimulation, *Mater. Sci. Eng. C Mater. Biol. Appl.* 32 (2012) 2163–2168.
- [9] K.E. Hammerick, A.W. James, Z. Huang, F.B. Prinz, M.T. Longaker, Pulsed direct current electric fields enhance osteogenesis in adipose-derived stromal cells, *Tissue Eng. Part A* 16 (2010) 917–931.
- [10] L. Petecchia, F. Sbrana, R. Utzeri, M. Vercellino, C. Usai, L. Visai, M. Vassalli, P. Gavazzo, Electro-magnetic field promotes osteogenic differentiation of BM-hMSCs through a selective action on Ca(2+)-related mechanisms, *Sci. Rep.* 5 (2015) 13856.
- [11] C. Daish, R. Blanchard, K. Fox, P. Pivonka, E. Pirogova, The application of pulsed electromagnetic fields (PEMFs) for bone fracture repair: past and perspective findings, *Ann. Biomed. Eng.* 46 (2018) 525–542.

- [12] F. Sahn, J. Ziebart, A. Jonitz-Heincke, D. Hansmann, T. Dauben, R. Bader, Alternating electric fields modify the function of human osteoblasts growing on and in the surroundings of titanium electrodes, *IJMS* 21 (2020) 6944.
- [13] D.J. Jiang, B.J. Shi, H. Ouyang, Y.B. Fan, Z.L. Wang, Z. Li, Emerging implantable energy harvesters and self-powered implantable medical electronics, *ACS Nano* 14 (2020) 6436–6448.
- [14] P.C. Tan, Q. Zheng, Y. Zou, B.J. Shi, D.J. Jiang, X.C. Qu, H. Ouyang, C.C. Zhao, Y. Cao, Y.B. Fan, Z.L. Wang, Z. Li, A battery-like self-charge universal module for motional energy harvest, *Adv. Energy Mater.* 9 (2019), 1901875.
- [15] Z.L. Wang, Triboelectric nanogenerators as new energy technology and self-powered sensors—principles, problems and perspectives, *Faraday Discuss.* 176 (2014) 447–458.
- [16] F.R. Fan, W. Tang, Z.L. Wang, Flexible nanogenerators for energy harvesting and self-powered electronics, *Adv. Mater.* 28 (2016) 4283–4305.
- [17] Z.L. Wang, J.H. Song, Piezoelectric nanogenerators based on zinc oxide nanowire arrays, *Science* 312 (2006) 242–246.
- [18] Z. Li, G. Zhu, R. Yang, A.C. Wang, Z.L. Wang, Muscle-driven in vivo nanogenerator, *Adv. Mater.* 22 (2010) 2534–2537.
- [19] Y. Liu, W. Liu, Z. Wang, W. He, Q. Tang, Y. Xi, X. Wang, H. Guo, C. Hu, Quantifying contact status and the air-breakdown model of charge-excitation triboelectric nanogenerators to maximize charge density, *Nat. Commun.* 11 (2020) 1599.
- [20] Q. Zheng, Q. Tang, Z.L. Wang, Z. Li, Self-powered cardiovascular electronic devices and systems, *Nat. Rev. Cardiol.* 18 (2021) 7–21.
- [21] Z. Liu, Q. Zheng, Y. Shi, L.L. Xu, Y. Zou, D.J. Jiang, B.J. Shi, X.C. Qu, H. Li, H. Ouyang, R.P. Liu, Y.X. Wu, Y.B. Fan, Z. Li, Flexible and stretchable dual mode nanogenerator for rehabilitation monitoring and information interaction, *J. Mater. Chem. B* 8 (2020) 3647–3654.
- [22] C. Zhao, H. Feng, L. Zhang, Z. Li, Y. Zou, P. Tan, H. Ouyang, D. Jiang, M. Yu, C. Wang, H. Li, L. Xu, W. Wei, Z. Li, Highly efficient in vivo cancer therapy by an implantable magnet triboelectric nanogenerator, *Adv. Funct. Mater.* 29 (2019), 1808640.
- [23] Z. Liu, L. Xu, Q. Zheng, Y. Kang, B. Shi, D. Jiang, H. Li, X. Qu, Y. Fan, Z.L. Wang, Z. Li, Human motion driven self-powered photodynamic system for long-term autonomous cancer therapy, *ACS Nano* 14 (2020) 8074–8083.
- [24] A.C. Wang, Z. Liu, M. Hu, C.C. Wang, X.D. Zhang, B.J. Shi, Y.B. Fan, Y.G. Cui, Z. Li, K.L. Ren, Piezoelectric nanofibrous scaffolds as in vivo energy harvesters for modifying fibroblast alignment and proliferation in wound healing, *Nano Energy* 43 (2018) 63–71.
- [25] G. Yao, L. Kang, J. Li, Y. Long, H. Wei, C.A. Ferreira, J.J. Jeffery, Y. Lin, W. Cai, X. Wang, Effective weight control via an implanted self-powered vagus nerve stimulation device, *Nat. Commun.* 9 (2018) 5349.
- [26] Q. Zheng, Y. Zou, Y. Zhang, Z. Liu, B. Shi, X. Wang, Y. Jin, H. Ouyang, Z. Li, Z. L. Wang, Biodegradable triboelectric nanogenerator as a life-time designed implantable power source, *Sci. Adv.* 2 (2016), e1501478.
- [27] H. Wang, J.H. Wang, T.Y.Y. He, Z. Li, C. Lee, Direct muscle stimulation using diode-amplified triboelectric nanogenerators (TEGs), *Nano Energy* 63 (2019), 103844.
- [28] J.H. Wang, T.Y.Y. He, C. Lee, Development of neural interfaces and energy harvesters towards self-powered implantable systems for healthcare monitoring and rehabilitation purposes, *Nano Energy* 65 (2019), 104039.
- [29] H. Ouyang, Z. Liu, N. Li, B.J. Shi, Y. Zou, F. Xie, Y. Ma, Z. Li, H. Li, Q. Zheng, X. C. Qu, Y.B. Fan, Z.L. Wang, H. Zhang, Z. Li, Symbiotic cardiac pacemaker, *Nat. Commun.* 10 (2019) 1821.
- [30] H. Ouyang, J.J. Tian, G.L. Sun, Y. Zou, Z. Liu, H. Li, L.M. Zhao, B.J. Shi, Y.B. Fan, Y. F. Fan, Z.L. Wang, Z. Li, Self-powered pulse sensor for antidiastole of cardiovascular disease, *Adv. Mater.* 29 (2017), 1703456.
- [31] G. Yao, D. Jiang, J. Li, L. Kang, S. Chen, Y. Long, Y. Wang, P. Huang, Y. Lin, W. Cai, X. Wang, Self-activated electrical stimulation for effective gair regeneration via a wearable omnidirectional pulse generator, *ACS Nano* 13 (2019) 12345–12356.
- [32] J. Tian, R. Shi, Z. Liu, H. Ouyang, M. Yu, C. Zhao, Y. Zou, D. Jiang, J. Zhang, Z. Li, Self-powered implantable electrical stimulator for osteoblasts' proliferation and differentiation, *Nano Energy* 59 (2019) 705–714.
- [33] R. Shi, J. Zhang, J. Tian, C. Zhao, Z. Li, Y. Zhang, Y. Li, C. Wu, W. Tian, Z. Li, An effective self-powered strategy to endow titanium implant surface with associated activity of anti-biofilm and osteogenesis, *Nano Energy* 77 (2020), 105201.
- [34] L. Leppik, K.M.C. Oliveira, M.B. Bhavsar, J.H. Barker, Electrical stimulation in bone tissue engineering treatments, *Eur. J. Trauma Emerg. Surg.* 46 (2020) 231–244.
- [35] P. Muller, U. Bulnheim, A. Diener, F. Luthen, M. Teller, E.D. Klinkenberg, H. G. Neumann, B. Nebe, A. Liebold, G. Steinhoff, J. Rychly, Calcium phosphate surfaces promote osteogenic differentiation of mesenchymal stem cells, *J. Cell. Mol. Med.* 12 (2008) 281–291.
- [36] S. Vimalraj, Alkaline phosphatase: structure, expression and its function in bone mineralization, *Gene* 754 (2020), 144855.



Yingzi Zhang received his Master's Degree and Ph.D. Degree from Soochow University. Assistant director physician, Dept. of the Orthopedics, the Second Affiliated Hospital of Soochow University, His research interests include the pathogenesis and treatment of osteoporosis.



Lingling Xu received her Bachelor's Degree and Master's Degree from the West China School of Pharmacy, Sichuan University. She is currently pursuing the Ph.D. degree at Beijing Institute of Nanoenergy and Nanosystems, Chinese Academy of Sciences. Her research interests include the stimulus responsive drug delivery system and selfpowered biomedical systems.



Dr. Zhuo Liu received his Ph.D. in Biomedical Engineering from Beihang University in 2020. He is currently doing post-doctoral research at Beijing Advanced Innovation Centre for Biomedical Engineering, Beihang University. His research interests are focusing on self-powered biomedical systems and measurement of cell traction force.



Xi Cui received her bachelor's degree from Jilin University in the Department of Life and Sciences, Jilin, China, in 2019. Now she is a master student in Beijing Institute of Nanoenergy and Nanosystems, Chinese Academy of Sciences. Her current research mainly focuses on nanogenerators and in vivo self-powered biosensors.



Zhuo Xiang received his Bachelor's Degree from School of Pharmacy, Hubei University of Chinese medicine. And received master's Degree in School of Pharmacy, Nanchang University. He is currently pursuing the Ph.D. degree at School of Physical Science and Technology, Guangxi University. His interest is major in the drug-controlled system.



Jinyu Bai, Ph.D. and Physician, Dept. of the Orthopedics, the Second Affiliated Hospital of Soochow University. His main research area: pathogenesis and treatment of bone degenerative diseases.



Zhe Li received her Ph.D. degree in Beijing Institute of Nanoenergy and Nanosystems, Chinese Academy of Sciences, in 2020. She is currently a post-doctoral researcher in Beijing Institute of Technology, Institute of Engineering Medicine, School of Life Science, Beijing, China. Her research work is focusing on the application of nanogenerator for self-powered biomedical systems, active sensors, and energy storage devices.



Dongjie Jiang received his bachelor's degree in Light Chemical Engineering (Excellence Program), Zhejiang Sci-Tech University in 2017. He is currently pursuing the Ph.D. degree with the Beijing Institute of Nanoenergy and Nanosystems, Chinese Academy of Sciences. His current interests include implantable self-powered systems and applications based on nanogenerators.



Yizhu Shan received her Bachelor's Degree from the School of Pharmacy, Harbin Medical University. She is currently pursuing the Ph.D. degree at Beijing Institute of Nanoenergy and Nanosystems, Chinese Academy of Sciences. Her research interests include developing novel therapy for nervous system injury and self-powered biomedical systems.



Jiangtao Xue received his Master's Degree from College of Mechanical Engineering and Applied Electronics Technology in Beijing University of Technology. He is currently pursuing the Ph.D. degree at Beijing Institute of Technology. His research interests include the self-powered devices and wearable electronics.



Yuan Yang received Bachelor's degree in Shanxi Datong University, and obtained Master's Degree in Beijing University of Chemical Technology. She is currently pursuing the Ph.D. degree at Beijing Institute of Nanoenergy and Nanosystems, Chinese Academy of Sciences. Her research work is focusing on drug delivery, biomolecule detection and the self-powered transdermal biomedical systems.



Chan Wang is currently a Ph.D. student in Beijing Institute of Nanoenergy and Systems, University of Chinese Academy of Sciences. She received his BS from China University of Geosciences, Wuhan in 2016. Her research focuses on the broad topics of materials science and engineering in human-machine interfaces including functionalization of soft materials, hydrogel bioelectronics.



Lin Bo received her Bachelor's Degree and Master's Degree from Nanjing Medical University, Ph.D. Degree from Soochow University. Assistant director physician, Dept. of the Rheumatology, the Second Affiliated Hospital of Soochow University. Her research interests include the bone metabolism and the mechanism and therapy of osteoporosis.



Dr. Youxi Lin received his M.D. from Peking Union Medical College, Chinese Academy of Medical Sciences in the department of orthopaedic surgery in 2020, and now works in Beijing Tiantan Hospital, Capital Medical University. His research work focuses on degenerative spinal disease and spinal deformity.



Prof. Zhou Li received his Ph.D. from Peking University in Department of Biomedical Engineering in 2010, and Bachelor's Degree from Wuhan University in 2004. He joined School of Biological Science and Medical Engineering of Beihang University in 2010 as an Associate Professor. Currently, he is a Professor in Beijing Institute of Nanoenergy and Nanosystems, Chinese Academy of Sciences. His research interests include nanogenerators, in vivo energy harvesters, self-powered medical devices, and biosensors.



Xiaozhong Zhou, Professor & Head, Dept. of the Orthopedics, the Second Affiliated Hospital of Soochow University, His research interests include mechanism and therapy of osteoporosis and spinal cord injury repair.